

Spectral and FTIR Analysis of Ho^{3+} ions doped Zinc Lithium Tungsten Aluminobismuth borate Glasses

S.L.Meena

Ceramic Laboratory, Department of physics, Jai Narain Vyas University, Jodhpur 342001 (Raj.) India

Abstract

Glass of the system: $(40-x)\text{Bi}_2\text{O}_3:10\text{ZnO}:10\text{Li}_2\text{O}:10\text{WO}_3:10\text{Al}_2\text{O}_3:20\text{B}_2\text{O}_3:x\text{Ho}_2\text{O}_3$ (where $x=1, 1.5, 2$ mol %) have been prepared by melt-quenching method. The amorphous nature of the prepared glass samples was confirmed by X-ray diffraction. Optical absorption, excitation, fluorescence and FTIR spectra were recorded at room temperature for all glass samples. Judd-Ofelt intensity parameters Ω_λ ($\lambda=2, 4$ and 6) are evaluated from the intensities of various absorption bands of optical absorption spectra. Using these intensity parameters various radiative properties like spontaneous emission probability (A), branching ratio (β), radiative life time (τ_R) and stimulated emission cross-section (σ_p) of various emission lines have been evaluated.

Keywords: ZLTABB Glasses, Optical Properties, FTIR Spectroscopy, Judd-Ofelt Theory, Transmittance Properties.

Date of Submission: 13-06-2022

Date of Acceptance: 27-06-2022

I. Introduction

Glasses doped with rare earth ions have attracted a great deal of attention because of their applications in laser fusion, optical fibers, sensors, infrared detectors, marine optical communications, up-conversion lasers, optical data storage and high density memory storage devices [1–5]. Among different glasses, bismuth borate glasses have unique properties. They have high transparency, high thermal stability and low dispersion rates. Borate glasses possess interesting properties like lower phonon energy, high density, high refractive indices, high gain density, high solubility, non-linear optical susceptibilities and low melting temperature [6–10]. Addition of network modifier (NMF) Li_2O to the bismuth borate glasses improves both electrical and mechanical properties of such glasses [11, 12]. ZnO is also added due to its specific chemical and microstructure properties. Despite, the Bi_2O_3 is not a classical network former, it exhibits some superior properties like high refractive index, high optical basicity and large polarizability [13]. Moreover, bismuth oxide contained host glass matrix improves chemical durability of the glass [14, 15].

The present work reports on the preparation and characterization of rare earth doped heavy metal oxide (HMO) glass systems for lasing materials. I have studied on the Optical absorption, excitation, fluorescence and FTIR spectra of Ho^{3+} doped zinc lithium tungsten aluminobismuth borate glasses. The intensities of the transitions for the rare earth ions have been estimated successfully using the Judd-Ofelt theory. The laser parameters such as radiative probabilities (A), branching ratio (β), radiative life time (τ_R) and stimulated emission cross section (σ_p) are evaluated using J.O. intensity parameters (Ω_λ , $\lambda=2, 4$ and 6).

II. Experimental Techniques

Preparation of glasses

The following Ho^{3+} doped bismuth borate glass samples $(40-x)\text{Bi}_2\text{O}_3:10\text{ZnO}:10\text{Li}_2\text{O}:10\text{WO}_3:10\text{Al}_2\text{O}_3:20\text{B}_2\text{O}_3:x\text{Ho}_2\text{O}_3$ (where $x=1, 1.5$ and 2 mol%) have been prepared by melt-quenching method. Analytical reagent grade chemical used in the present study consist of Bi_2O_3 , ZnO , Li_2O , WO_3 , Al_2O_3 , B_2O_3 and Ho_2O_3 . They were thoroughly mixed by using an agate pestle mortar. then melted at 985°C by an electrical muffle furnace for 2h., After complete melting, the melts were quickly poured in to a preheated stainless steel mould and annealed at temperature of 250°C for 2h to remove thermal strains and stresses. Every time fine powder of cerium oxide was used for polishing the samples. The glass samples so prepared were of good optical quality and were transparent. The chemical compositions of the glasses with the name of samples are summarized in **Table 1**.

Table 1.

Chemical composition of the glasses

Sample	Glass composition (mol %)
ZLTABB(UD)	40Bi ₂ O ₃ :10ZnO:10Li ₂ O:10WO ₃ :10Al ₂ O ₃ :20B ₂ O ₃
ZLTABB (HO1)	39Bi ₂ O ₃ :10ZnO:10Li ₂ O:10WO ₃ :10Al ₂ O ₃ :20B ₂ O ₃ :1 Ho ₂ O ₃
ZLTABB(HO1.5)	38.5Bi ₂ O ₃ :10ZnO:10Li ₂ O:10WO ₃ :10Al ₂ O ₃ :20B ₂ O ₃ :1.5Ho ₂ O ₃
ZLTABB(HO2)	38Bi ₂ O ₃ :10ZnO:10Li ₂ O:10WO ₃ :10Al ₂ O ₃ :20B ₂ O ₃ :2Ho ₂ O ₃

ZLTABB (UD) -Represents undoped Zinc Lithium Tungsten AluminoBismuth Borateglass specimens

ZLTABB(HO)-Represents Ho^{3+} doped Zinc Lithium Tungsten AluminoBismuth Borateglass specimens

III. Theory

3.1 Oscillator Strength

The intensity of spectral lines are expressed in terms of oscillator strengths using the relation [16].

$$f_{\text{expt.}} = 4.318 \times 10^{-9} \int \varepsilon(\nu) d\nu \quad (1)$$

where, $\varepsilon(\nu)$ is molar absorption coefficient at a given energy ν (cm^{-1}), to be evaluated from Beer–Lambert law. Under Gaussian Approximation, using Beer–Lambert law, the observed oscillator strengths of the absorption bands have been experimentally calculated [17], using the modified relation:

$$P_m = 4.6 \times 10^{-9} \times \frac{1}{cl} \log \frac{I_0}{I} \times \Delta\nu_{1/2} \quad (2)$$

where c is the molar concentration of the absorbing ion per unit volume, l is the optical path length, $\log I_0/I$ is optical density and $\Delta\nu_{1/2}$ is half band width.

3.2. Judd-Ofelt Intensity Parameters

According to Judd[18] and Ofelt[19] theory, independently derived expression for the oscillator strength of the induced forced electric dipole transitions between an initial J manifold $|4f^N(S, L) J\rangle$ level and the terminal J' manifold $|4f^N(S', L') J'\rangle$ is given by:

$$\frac{8\pi^2 mc \nu}{3h(2J+1)n} \frac{1}{n} \left[\frac{(n^2+2)^2}{9} \right] \times S(J, J') \quad \text{Where, the} \quad (3)$$

line strength $S(J, J')$ is given by the equation

$$S(J, J') = e^2 \sum_{\lambda} \Omega_{\lambda} \langle 4f^N(S, L) J \| U^{(\lambda)} \| 4f^N(S', L') J' \rangle^2 \quad (4)$$

$\lambda = 2, 4, 6$

In the above equation m is the mass of an electron, c is the velocity of light, ν is the wave number of the transition, h is Planck's constant, n is the refractive index, J and J' are the total angular momentum of the initial and final level respectively, Ω_{λ} ($\lambda = 2, 4$ and 6) are known as Judd-Ofelt intensity.

3.3 Radiative Properties

The Ω_{λ} parameters obtained using the absorption spectral results have been used to predict radiative properties such as spontaneous emission probability (A) and radiative life time (τ_R), and laser parameters like fluorescence branching ratio (β_R) and stimulated emission cross section (σ_p).

The spontaneous emission probability from initial manifold $|4f^N(S', L') J'\rangle$ to a final manifold $|4f^N(S, L) J\rangle$ is given by:

$$A[(S', L') J'; (S, L) J] = \frac{64 \pi^2 \nu^3}{3h(2J'+1)} \left[\frac{n(n^2+2)^2}{9} \right] \times S(J', J) \quad (5)$$

$$\text{Where, } S(J', J) = e^2 [\Omega_2 \| U^{(2)} \|^2 + \Omega_4 \| U^{(4)} \|^2 + \Omega_6 \| U^{(6)} \|^2]$$

The fluorescence branching ratio for the transitions originating from a specific initial manifold $|4f^N(S', L') J'\rangle$ to a final many fold $|4f^N(S, L) J\rangle$ is given by

$$\beta[(S', L') J'; (S, L) J] = \frac{A[(S', L) J]}{\sum_{A[(S', L') J'(\bar{S}, \bar{L})]} A[(S', L) J]} \quad (6)$$

S L J

where, the sum is over all terminal manifolds.

The radiative life time is given by

$$\tau_{rad} = \sum A[(S', L') J'; (S, L)] = A_{Total}^{-1} \quad (7)$$

S L J

where, the sum is over all possible terminal manifolds. The stimulated emission cross-section for a transition from an initial manifold $|4f^N(S', L') J\rangle$ to a final manifold $|4f^N(S, L) J\rangle$ is expressed as

$$\sigma_p(\lambda_p) = \left[\frac{\lambda_p^4}{8\pi c n^2 \Delta\lambda_{eff}} \right] \times A[(S', L') J'; (\bar{S}, \bar{L}) \bar{J}] \quad (8)$$

where, λ_p the peak fluorescence wavelength of the emission band and $\Delta\lambda_{eff}$ is the effective fluorescence line width.

3.4 Nephelauxetic Ratio (β') and Bonding Parameter ($b^{1/2}$)

The nature of the R-O bond is known by the Nephelauxetic Ratio (β') and Bonding Parameters ($b^{1/2}$), which are computed by using following formulae [20, 21]. The Nephelauxetic Ratio is given by

$$\beta' = \frac{\nu_g}{\nu_a} \quad (9)$$

where, ν_a and ν_g refer to the energies of the corresponding transition in the glass and free ion, respectively. The value of bonding parameter ($b^{1/2}$) is given by

$$b^{1/2} = \left[\frac{1-\beta'}{2} \right]^{1/2} \quad (10)$$

IV. Result and Discussion

4.1 XRD Measurement

Figure 1 presents the XRD pattern of the sample contain $-\text{Bi}_2\text{O}_3$ which is show no sharp Bragg's peak, but only a broad diffuse hump around low angle region. This is the clear indication of amorphous nature within the resolution limit of XRD instrument.

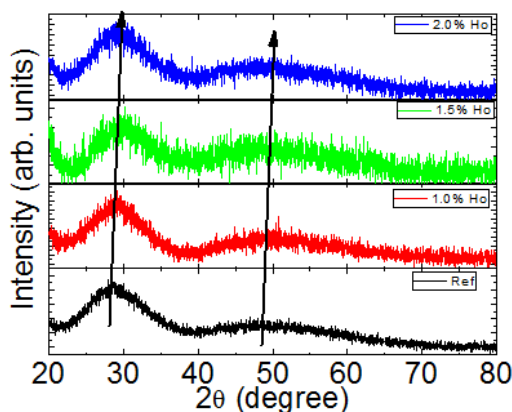


Fig. 1 X-ray diffraction pattern of ZLTABB (HO) Glasses.

4.2 FTIR Transmission spectra

The FTIR spectrum of ZLTABB (HO 01) glass in the wave number range $500-2500\text{cm}^{-1}$ is presented in Fig.2 and the possible mechanism bands are tabulated in Table 2.

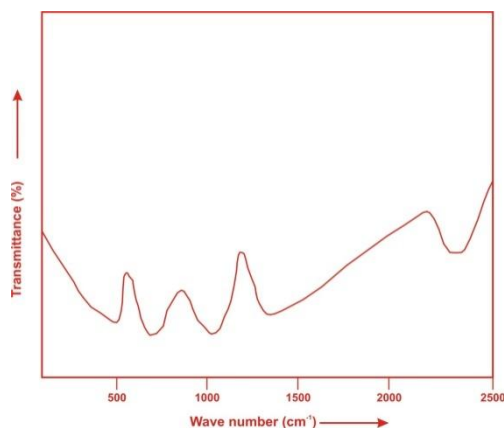


Fig. (2) FTIR spectrum of ZLTABB HO (01) glass.

In the studied glasses, the IR features located below 600 cm^{-1} are attributed to BiO bonds in $[\text{BiO}_6]$ so the band observed at 510 cm^{-1} is attributed to BiO bonds in BiO_6 [22]. The observed band around at 702 cm^{-1} is due to the bending vibration of B-O-B linkage in borate network[23] whereas the band at 1025 cm^{-1} is due to asymmetric stretching vibrations of the B-O bonds in BO_4 units [23] and the broad band at 1335 cm^{-1} is attributed to the B-O bonds due to stretching vibrations of trigonal BO_3 units in the borate network [24]. The observed band around at 2350 cm^{-1} is attributed to water groups OH stretching vibrations [25].

Table2. Assignment of infrared transmission bands of(ZLTABBHO 01) glass.

Peak position(cm^{-1})	Band Assignment
~ 510	Bi-O bonds in BiO_6 Units
~702	Bending vibrations of B-O-B linkage
~1025	B-O Stretching vibrations of BO_4 tetrahedral
~1335	B-O Stretching vibrations of the trigonal BO_3 units
~2350	Presence of hydrogen bonding

4.3 Absorption Spectrum

The absorption spectra of Ho^{3+} doped ZLTABB glass specimens have been presented in Figure 3 in terms of optical density versus wavelength. Twelve absorption bands have been observed from the ground state $^5\text{I}_8$ to excited states $^5\text{I}_5$, $^5\text{I}_4$, $^5\text{F}_5$, $^5\text{F}_4$, $^5\text{F}_3$, $^3\text{K}_8$, $^5\text{G}_6$, ($^5\text{G}_3, ^3\text{G}_5$), $^5\text{G}_4$, $^5\text{G}_2$, $^5\text{G}_3$, and $^3\text{F}_4$ for Ho^{3+} doped ZLTABB glasses.

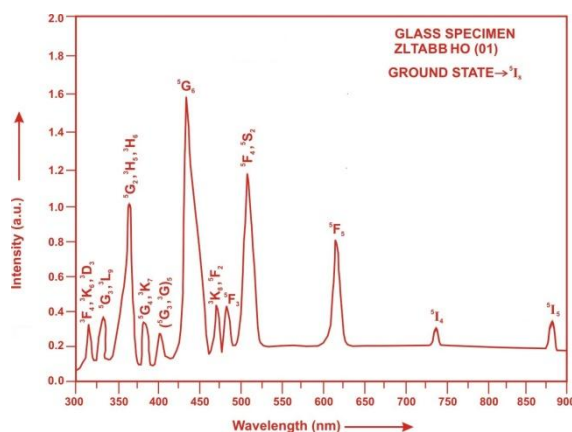


Fig. (3) Absorption spectrum of ZLTABB HO (01) glass.

The experimental and calculated oscillator strength for Ho^{3+} ions in ZLTABB glasses are given in **Table 3**.

Table 3: Measured and calculated oscillator strength ($P_m \times 10^{+6}$) of Ho^{3+} ions in ZLTABB glasses.

Energy level from $^5\text{I}_8$	Glass ZLTABB(HO01)		Glass ZLTABB(HO1.5)		Glass ZLTABB(HO02)	
	P_{exp}	P_{cal}	P_{exp}	P_{cal}	P_{exp}	P_{cal}
$^5\text{I}_5$	0.42	0.24	0.38	0.24	0.35	0.23
$^5\text{I}_4$	0.05	0.02	0.04	0.02	0.03	0.02
$^5\text{F}_5$	3.62	2.78	3.58	2.70	3.52	2.67
$^5\text{F}_4$	4.58	4.32	4.52	4.21	4.48	4.17

⁵ F ₃	1.52	2.39	1.48	2.34	1.42	2.32
³ K ₈	1.38	1.98	1.32	1.90	1.28	1.88
⁵ G ₆	26.68	26.70	22.96	22.98	23.23	22.28
(² G ₃ , ³ G ₅)	3.72	1.70	3.68	1.63	3.61	1.60
⁵ G ₄	0.06	0.61	0.05	0.58	0.04	0.58
⁵ G ₂	5.76	5.63	5.72	4.95	5.68	4.82
⁵ G ₃	1.46	1.41	1.42	1.33	1.38	1.31
³ F ₄	1.32	4.17	1.27	4.00	1.22	3.94
r.m.s. deviation	±1.0984		±1.1006		±1.0986	

Computed values of F₂, Lande' parameter (ξ_{4f}), Nephelauxetic ratio(β') and bonding parameter(b^{1/2}) for Ho³⁺ ions in ZLTABB glass specimen are given in Table 3.

Table 3: F₂, ξ_{4f}, β' and b^{1/2} parameters for Holmium doped glass specimen.

Glass Specimen	F ₂	ξ _{4f}	β'	b ^{1/2}
Ho ³⁺	358.82	1258.16	0.9337	0.1821

In the Zinc Lithium Tungsten Aluminobismuth Borate glasses (ZLTABB) Ω₂, Ω₄ and Ω₆ parameters decrease with the increase of x from 1 to 2 mol%. The order of magnitude of Judd-Ofelt intensity parameters is Ω₂ > Ω₆ > Ω₄ for all the glass specimens. The spectroscopic quality factor (Ω₄/Ω₆) related with the rigidity of the glass system has been found to lie between 0.597 and 0.617 in the present glasses.

The values of Judd-Ofelt intensity parameters are given in Table 4.

Table 4: Judd-Ofelt intensity parameters for Ho³⁺ doped ZLTABB glass specimens.

Glass Specimen	Ω ₂ (pm ²)	Ω ₄ (pm ²)	Ω ₆ (pm ²)	Ω ₄ /Ω ₆	Ref.
ZLTABB (HO01)	5.911	1.210	1.962	0.6167	P.W.
ZLTABB (HO1.5)	4.958	1.155	1.917	0.6019	P.W.
ZLTABB (HO02)	4.785	1.134	1.901	0.5965	P.W.
TFB(EU)	4.76	1.09	3.09	0.353	[26]
ZABS(EU)	5.253	1.446	2.750	0.526	[27]
LCASO(HO)	5.606	1.175	1.981	0.593	[28]
LLBP (TB)	3.339	1.179	2.462	0.479	[29]
BBFB(ER)	3.302	0.845	1.09	0.775	[30]

4.4 Excitation Spectrum

The Excitation spectrum of ZLTABB (HO 01) glass has been presented in Figure 4 in terms of Excitation Intensity versus wavelength. The excitation spectrum was recorded in the spectral region 325–525 nm fluorescence at 545nm having different excitation band centered at 349, 419, 452, 473 and 486 nm are attributed to the ⁵G₃, (²G₃, ³G₅), ⁵G₆, ³K₈ and ²F₃ transitions, respectively. The highest absorption level is ⁵G₆ and is at 452nm. So this is to be chosen for excitation wavelength.

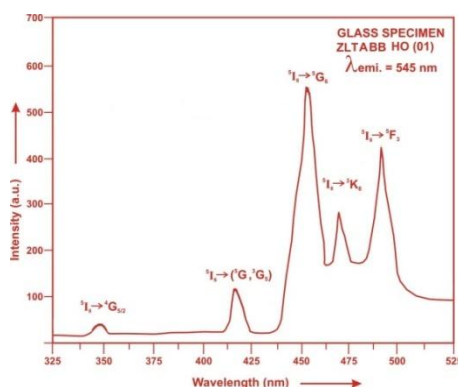


Fig. (4) Excitation spectrum of ZLTABB HO (01) glass.

4.5 Fluorescence Spectrum

The fluorescence spectrum of Ho³⁺ doped in zinc lithium tungsten aluminobismuth borate glass is shown in Figure 5. There are eleven broad bands observed in the Fluorescence spectrum of Ho³⁺ doped zinc lithium tungsten aluminobismuth borate glass. The wavelengths of these bands along with their assignments are given in Table 5. The peak with maximum emission intensity appears at 2035nm and corresponds to the (⁵I₇ → ⁵I₈) transition.

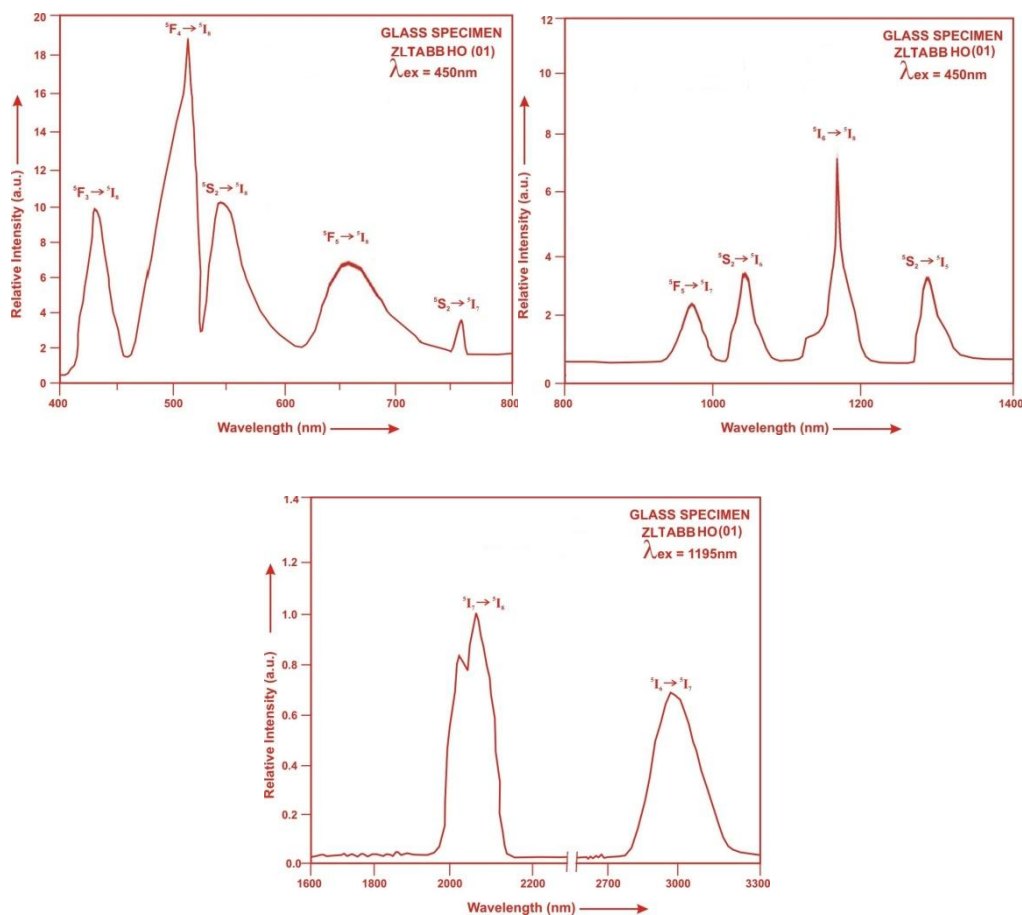


Fig. (5). Fluorescence spectrum of ZLTABB HO (01) glass.

Table 5: Emission peak wave lengths (λ_p), radiative transition probability (A_{rad}), branching ratio (β), stimulated emission cross-section (σ_p) and radiative life time (τ_R) for various transitions in Ho³⁺ doped ZLTABB glasses.

Transition	ZLTABB (HO 01)					ZLTABB (HO 1.5)				ZLTABB (HO 02)			
	λ_{max} (nm)	$A_{rad}(s^{-1})$	β	$\sigma_p(10^{-20} cm^2)$	$\tau_R(\mu s)$	$A_{rad}(s^{-1})$	β	$\sigma_p(10^{-20} cm^2)$	$\tau_R(\mu s)$	$A_{rad}(s^{-1})$	β	$\sigma_p(10^{-20} cm^2)$	$\tau_R(10^{-20} cm^2)$
$^5F_3 \rightarrow ^5I_8$	435	4831.78	0.2482	0.601		4734.50	0.2489	0.583		4699.58	0.2491	0.568	
$^5F_4 \rightarrow ^5I_8$	501	7679.50	0.3945	1.249		7496.45	0.3941	1.203		7431.59	0.3940	1.162	
$^5S_2 \rightarrow ^5I_8$	555	2014.67	0.1035	0.436		1975.37	0.1039	0.424		1961.67	0.1040	0.416	
$^5F_5 \rightarrow ^5I_8$	652	2190.07	0.1125	0.741		2129.90	0.1120	0.714		2107.18	0.1117	0.696	
$^5S_2 \rightarrow ^5I_7$	761	1528.83	0.0785	1.136		1498.21	0.0788	1.106		1487.01	0.0788	1.079	5301.99
$^5F_5 \rightarrow ^5I_7$	995	513.50	0.0264	1.229	5136.68	493.59	0.0260	1.165	5257.51	487.69	0.0259	1.130	
$^5I_6 \rightarrow ^5I_8$	1032	234.87	0.0121	0.706		229.59	0.0121	0.685		227.76	0.0121	0.666	
$^5S_2 \rightarrow ^5I_5$	1195	268.89	0.0138	1.227		261.97	0.0138	1.181		259.73	0.0138	1.151	
$^5S_2 \rightarrow ^5I_6$	1310	71.51	0.0037	0.633		70.00	0.0037	0.610		69.48	0.0037	0.592	
$^5I_7 \rightarrow ^5I_8$	2035	106.88	0.0055	4.732		103.95	0.0055	4.568		103.02	0.0055	4.437	
$^5I_6 \rightarrow ^5I_7$	2925	27.32	0.0014	3.928		26.40	0.0014	3.755		26.13	0.0014	3.678	

V. Conclusion

In the present study, the glass samples of composition (40-x)Bi₂O₃:10ZnO:10Li₂O:10WO₃:10Al₂O₃:20B₂O₃:xHo₂O₃ (where x = 1, 1.5 and 2 mol %) have been prepared by melt-quenching method. The value of stimulated emission cross-section (σ_p) is found to be maximum for the transition ($^5F_4 \rightarrow ^5I_8$) for glass ZLTABB(HO 01), suggesting that glass ZLTABB (HO 01) is better compared to the other two glass systems ZLTABB (HO1.5) and ZLTABB(HO02). The large stimulated emission cross section in bismuth borate glasses suggests the possibility of utilizing these systems as laser materials. The FTIR of glasses revealed the presence of characteristic bonding vibrations of different functional groups.

References

- [1]. Kashif, I., Ratep, A. and Ahmed, S. (2020). Spectroscopic properties of lithium borate glass containing Sm³⁺ and Nd³⁺ ions, *Int. J. of Adv. in App. Sci.* 9(3), 211-219.
- [2]. Barbia, S., Mugonib, C., Montorsic, M., Affatigatod, M., Gattoe, C. and Siligardib, C. (2018). Structural and optical properties of cerium oxide doped barium bismuth borate glasses, *J. of Non-Cryst. Solids*, 499(1), 1-21.
- [3]. Balakrishna, A., Rajesh, D. and Ratnakaram, Y. C. (2013). Structural and optical properties of Nd³⁺ in lithium fluoro-borate glass with relevant modifier oxide. *Opt. Mater.* 35, 2670-2676.
- [4]. Anjaiah, J., Laxmikanth, C. and Veeraiah, N. (2014). Spectroscopic properties and luminescence behavior of europium doped lithium borate glasses. *Physica B: Cond. Matt.* 454, 148-156.
- [5]. Hassaan, M. Y., Saudi, H. A., Gomaa, H. M. and Morsy, A. S. (2020). Optical Properties of Bismuth Borate Glasses Doped with Zinc and Calcium Oxides, *J. of Mat. and App.* 9(1), 46-54.
- [6]. Rajesh, D., Balakrishna, A. and Ratnakaram, Y. C. (2012). Luminescence, structural and dielectric properties of Sm³⁺ impurities in strontium lithium bismuth borate glasses. *Opt. Mat.* 35, 108-116.
- [7]. Rao, S. L. S., Ramadevudu, G., Md. Shareefuddin, Hameed, A., Chary, M. N. and Rao, M. L. (2012). Optical properties of alkaline earth borate glasses, *Int. J. of Eng. Sci. and Tech.* 4(4), 25-35.
- [8]. Rajasree, Ch. and Krishna Rao, D. (2011). Spectroscopic investigations on alkali bismuth borate glasses doped with CuO. *J. Non-Cryst. Solids*, 357, 836-841.
- [9]. Ramadevudu, G., Laxmi Srinivasa Rao, S., Abdul Hameed, Shareefuddin, Md and Narasimha Chary, M. (2011). FTIR and some physical properties of alkaline earth borate glasses containing heavy metal oxides, *Int. J. of Eng. Sci. and Tech.* 3(9), 6698-7005.
- [10]. Yasser, B., Saddeek, E. R., S., El Sayed Moustafa, Hesham and Moustafa, M. (2008). Spectroscopic properties, electronic polarizability, and optical basicity of Bi₂O₃-Li₂O-B₂O₃ glasses, *Physica B: Condensed Matter*, 403, 13, 2399-2407.
- [11]. Devi, R. and Jayasankar, C. K. (1995). Optical properties of Nd³⁺ ions in lithium borate glasses, *Materials chemistry and physics*, 42, 106-119.
- [12]. Anjaiah, J. and Laxmikanth, C. (2015). Optical Properties of Neodymium Ion Doped Lithium Borate Glasses, 5, 173-183.
- [13]. Peng, M. and Wondraczek, L. (2009). Bismuth-Doped Oxide Glasses as Potential Solar Spectral Converters and Concentrators, *J. Mater. Chem.*, 19, 627-630.
- [14]. Ramteke, D. D., Annapurna, K., Deshpande, V. K. and Gedam, R. S. (2014). Effect of Nd³⁺ on spectroscopic properties of lithium borate glasses, *J. Rare Earths*, 32(12), 1148-1153.
- [15]. Dumbaugh, W. H. and Lapp, J. C. (1992). Heavy-Metal Oxide Glass, *J. Am. Cer. Soc.*, 75, 2315.
- [16]. Gorller-Walrand, C. and Binnemans, K. (1988). Spectral Intensities of f-f Transition. In: Gshneidner Jr., K. A. and Eyring, L., Eds., *Handbook on the Physics and Chemistry of Rare Earths*, Vol. 25, Chap. 167, North-Holland, Amsterdam, 101-264.
- [17]. Sharma, Y. K., Surana, S. S. L. and Singh, R. K. (2009). Spectroscopic Investigations and Luminescence Spectra of Sm³⁺ Doped Soda Lime Silicate Glasses. *Journal of Rare Earths*, 27, 773-780.
- [18]. Judd, B. R. (1962). Optical Absorption Intensities of Rare Earth Ions. *Physical Review*, 127, 750-761.
- [19]. Ofelt, G. S. (1962). Intensities of Crystal Spectra of Rare Earth Ions. *The Journal of Chemical Physics*, 37, 511.
- [20]. Sinha, S. P. (1983). Systematics and properties of lanthanides, Reidel, Dordrecht. 1-8.
- [21]. Krupke, W. F. (1974). *IEEE J. Quantum Electron QE*, 10, 450.
- [22]. Zheng, H., Xu, R., Mackenzie, J. D. (1989). Glass formation and glass structure of BiO_{1.5}-CuO-Ca_{0.5}Sr_{0.5}O system. *J Mater Res* 4, 911-915.
- [23]. H. Doweidar, Yasser B. Saddeek, FTIR and ultrasonic investigations on modified bismuth borate glasses, *J. Non-Cryst. Solids* 355 (2009) 348-354.
- [24]. Pisarski, W. A., Pisarska, J., Dominiak-Dzik, G., Ryba Romanowski, W. (2004). Visible and infrared spectroscopy of Pr³⁺ and Tm³⁺ ions in lead borate glasses. *J. Phys. Condens Matter* 16, 6171-6184.
- [25]. Scholzelt, H. (1991). *Glass Nature Structure and Properties*, Springer Verlag, New York.
- [26]. Kumar, R. V., Maheshvaran, K., Sudarsan, V. and Marimuthu, K. (2014). Concentration dependent luminescence studied on Eu³⁺ doped tellurofluoroborate glasses, *J. Lumin.*, 154, 160-167.
- [27]. Monisha, M., Murari, M. S., Sayyed, M. I., Ghamdi, H. A., Almuqrin, H. A., Lakshminarayana, G. and Kamath, S. D. (2021). Thermal, Structural and optical behavior of Eu³⁺ ions in Zinc AluminoBoro-Silicate glasses for bright red emissions, *Mat. Chem. and Phys.*, 270, 124787, 1-10.
- [28]. Meena, S. L. (2019). Spectral and Thermal properties of Ho³⁺ doped oxy-fluoride glasses, *Int. J. Eng. Res. and Manag. Studies*, 6(11), 1-8.
- [29]. Meena, S. L. (2018). Spectral and Thermal Properties of Tb³⁺ Doped in Lead Lithium Borophosphate Glasses. *I.J.C.P.S.* Vol. 7, No. 6, 1-8.
- [30]. Mariselvam, K. and Kumar, R. A. (2021). The emission characteristics of Er³⁺: BBFB glasses for infra-red laser and gamma ray shielding applications, *Optik: Int. J. for light and Elect. Optics*, 226, 165910, 1-17.

S.L.Meena. "Spectral and FTIR Analysis of Ho³⁺ ions doped Zinc Lithium Tungsten Alumino Bismuth borate Glasses." *International Journal of Engineering Science Invention (IJESI)*, Vol. 11(06), 2022, PP 57-63. Journal DOI- 10.35629/6734